



## Get Clarity On Generics

Cost-Effective CT & MRI Contrast Agents

 **FRESENIUS  
KABI**

[WATCH VIDEO](#)

# AJNR

This information is current as  
of August 12, 2025.

## **Diagnostic Accuracy of PET, SPECT, and Arterial Spin-Labeling in Differentiating Tumor Recurrence from Necrosis in Cerebral Metastasis after Stereotactic Radiosurgery**

G. Lai, A. Mahadevan, D. Hackney, P.C. Warnke, F. Nigim,  
E. Kasper, E.T. Wong, B.S. Carter and C.C. Chen

*AJNR Am J Neuroradiol* 2015, 36 (12) 2250-2255

doi: <https://doi.org/10.3174/ajnr.A4475>

<http://www.ajnr.org/content/36/12/2250>

# Diagnostic Accuracy of PET, SPECT, and Arterial Spin-Labeling in Differentiating Tumor Recurrence from Necrosis in Cerebral Metastasis after Stereotactic Radiosurgery

G. Lai, A. Mahadevan, D. Hackney, P.C. Warnke, F. Nigim, E. Kasper, E.T. Wong, B.S. Carter, and C.C. Chen



## ABSTRACT

**BACKGROUND AND PURPOSE:** Radiographic assessment of cerebral metastasis after stereotactic radiosurgery remains a major challenge in neuro-oncology. It is often difficult to distinguish tumor progression from radiation necrosis in this setting using conventional MR imaging. The objective of this study was to compare the diagnostic sensitivity and specificity of different functional imaging modalities for detecting tumor recurrence after stereotactic radiosurgery.

**MATERIALS AND METHODS:** We retrospectively reviewed patients treated between 2007 and 2010 and identified 14 patients with cerebral metastasis who had clinical or radiographic progression following stereotactic radiosurgery and were imaged with arterial spin-labeling, FDG-PET, and thallium SPECT before stereotactic biopsy. Diagnostic accuracy, specificity, sensitivity, positive predictive value, and negative predictive value were calculated for each imaging technique by using the pathologic diagnosis as the criterion standard.

**RESULTS:** Six patients (42%) had tumor progression, while 8 (58%) developed radiation necrosis. FDG-PET and arterial spin-labeling were equally sensitive in detecting tumor progression (83%). However, the specificity of arterial spin-labeling was superior to that of the other modalities (100%, 75%, and 50%, respectively). A combination of modalities did not augment the sensitivity, specificity, positive predictive value, or negative predictive value of arterial spin-labeling.

**CONCLUSIONS:** In our series, arterial spin-labeling positivity was closely associated with the pathologic diagnosis of tumor progression after stereotactic radiosurgery. Validation of this finding in a large series is warranted.

**ABBREVIATIONS:** ASL = arterial spin-labeling; CE = contrast-enhanced; NPV = negative predictive value; PPV = positive predictive value; RN = radiation necrosis; SRS = stereotactic radiosurgery; SUV = standard uptake value; TP = tumor progression

Stereotactic radiosurgery (SRS) has emerged as an important treatment technique for patients with cerebral metastasis. A major challenge in the clinical management of these patients involves determination of tumor response to treatment.<sup>1</sup> Radiographically, SRS can induce reactive changes in the irradiated volume and edema in the surrounding cerebrum. These changes lead to breakdown of the blood-brain barrier, resulting in contrast enhancement on conventional MR imaging.<sup>2-4</sup> This phenomenon, termed “radiation necrosis” (RN), is often difficult to distin-

guish from tumor progression (TP) by using standard contrast-enhanced MR imaging (CE-MR imaging). Patients with RN are treated with steroids, anticoagulants, hyperbaric oxygen, or anti-angiogenic therapy, while patients with TP require either surgical intervention or chemotherapy.<sup>5,6</sup> Thus, the ability to distinguish RN from TP fundamentally drives clinical decision-making and patient care.


Currently, patients with radiographically ambiguous lesions undergo surgical biopsy or resection.<sup>5</sup> While these procedures are generally safe, morbidity ranges from 1% to 9%.<sup>7-9</sup> Most often, the morbidities involve transient neurologic deficits, but rare devastating neurologic consequences and death have also been reported.<sup>7-9</sup> In this context, there is a critical need for noninvasive modalities that would allow reliable discrimination of RN from TP.

Advances in physiologic imaging hold promise as alternate modalities to aid in the discrimination of RN from TP. Rather than relying on contrast extravasation, such imaging is based on the principle of measuring differences in physiologic states between proliferative tumor tissue and normal cerebrum. To the extent that RN and TP exhibit distinct metabolic states, physio-

Received February 21, 2015; accepted after revision May 3.

From the School of Medicine (G.L., B.S.C., C.C.C.), University of California, San Diego, La Jolla, California; Departments of Radiation Oncology (A.M.) and Radiology (D.H.), Division of Neurosurgery (F.N., E.K.), and Department of Neurology (E.T.W.), Beth Israel Deaconess Medical Center, Harvard Medical School, Boston, Massachusetts; and Division of Neurosurgery (P.C.W.), University of Chicago, Chicago, Illinois.

Please address correspondence to Clark C. Chen, MD, PhD, Division of Neurosurgery, University of California, San Diego, 3855 Health Science Dr, No. 0987, La Jolla, CA 92093-0987; e-mail: clarkchen@ucsd.edu

 Indicates article with supplemental on-line table.

<http://dx.doi.org/10.3174/ajnr.A4475>

**Table 1: Demographic information, clinical course, location of tumor, radiation dose, time between SRS and follow-up imaging, biopsy results, and imaging results of each patient<sup>a</sup>**

Pt	Age (yr)	Clinical Course	Location	SRS Dose	SRS to Imaging	Bx	PET	SPECT	MR ASL
1	69	RCC, s/p SRS and stent, new CE	Left paraventricular	22 Gy × 1	11 Mo	RN	Negative	Positive	Negative
2	63	NSCLC, s/p SRS, new CE	Right frontal	19 Gy × 1	12 Mo	TP	SUV 20	Positive	Positive
3	79	NSCLC, s/p SRS, neurologic deterioration	Right frontal	22 Gy × 1	8 Mo	RN	SUV 4.9	Negative	Negative
4	64	Esophageal cancer, s/p SRS, new CE	Left frontal	21 Gy × 1	4 Mo	TP	Negative	Positive	Positive
5	72	SCLC, 3 lesions s/p WBRT + SRS	Left parietal	22 Gy × 1	7 Mo	TP	SUV 10.3	Positive	Positive
6	46	Breast cancer, s/p SRS, new CE	Right cerebellar	22 Gy × 1	4 Mo	TP	SUV 6.6	Negative	Positive
7	65	Melanoma, s/p SRS, neurologic decline	Right temporal	18 Gy × 1	10 Mo	RN	SUV 7.2	Positive	Negative
8	63	RCC, s/p SRS, new CE	Right thalamus	16 Gy × 1	6 Mo	RN	Negative	Negative	Negative
9	58	Melanoma, s/p IR, enlarged CE	Right frontal	19 Gy × 1	4 Mo	TP	SUV 10.7	Negative	Negative
10	52	NSCLC, s/p SRS, new CE	Right cerebellar	18 Gy × 1	3 Mo	RN	Negative	Positive	Negative
11	59	Melanoma, s/p SRS	Left frontal	22 Gy × 1	3 Mo	TP	SUV 8	Negative	Positive
12	52	Breast cancer, s/p SRS	Right temporal	8 Gy × 3	11 Mo	RN	Negative	Negative	Negative
13	56	RCC, s/p SRS	Left temporal	21 Gy × 1	12 Mo	RN	Negative	Negative	Negative
14	49	Melanoma, s/p SRS	Right frontal	21 Gy × 1	8 Mo	RN	Negative	Negative	Negative

**Note:**—RCC indicates renal cell carcinoma; Bx, biopsy; s/p, status-post; IR, ionizing radiation; NSCLC, non-small cell lung cancer; SCLC, small cell lung cancer; WBRT, whole brain radiation therapy.

<sup>a</sup> Patients 1, 6, and 9 are those featured in the illustrative cases. Cells next to patients 1, 3, 7, 8, 10, and 12–14 represent RN on biopsy; other cells represent TN.

logic imaging may better distinguish these phenomena than structural imaging.

The objective of the current study was to compare the diagnostic utility of FDG-PET, thallium SPECT, and arterial spin-labeling (ASL)-MR imaging in the setting of brain metastasis with progression on CE-MR imaging after SRS treatment. We retrospectively identified patients with a definitive pathologic diagnosis who underwent FDG-PET, thallium SPECT, and ASL before stereotactic biopsy. Most important, biopsies were targeted to regions of positive signals in these modalities. Sensitivity, specificity, positive predictive value, and negative predictive values were calculated.

## MATERIALS AND METHODS

### Patients

This research was approved by the Beth Israel Deaconess Medical Center, Harvard Medical School Institutional Review Board (IRB 2010-P-000134). The cohort of 267 consecutively biopsied patients from 2007 to 2011 was previously described.<sup>10</sup> The inclusion criteria for this study were the following patients: 1) those who underwent stereotactic radiosurgery; 2) had radiographic progression on conventional CE-MR imaging accompanied by clinical deterioration; 3) underwent FDG-PET, thallium SPECT, and ASL-MR imaging before biopsy; and 4) had a definitive tissue diagnosis after biopsy. Patients underwent physiologic imaging studies and biopsy after review of a brain tumor board consisting of 3 neurosurgeons, 2 radiation oncologists, 2 neuro-oncologists, a neuroradiologist, and a neuropathologist. Patient characteristics are summarized in Table 1.

### Image Acquisition and Interpretation

All images were reviewed by a board-certified neuroradiologist as a part of standard patient care. Radiologists interpreting functional results were not precluded from comparing any one study with studies acquired previously. MR images were acquired on a Signa HDx 3T scanner (GE Healthcare, Milwaukee, Wisconsin) with standard T2-weighted, FLAIR, and T1 sequences. Contrast-enhanced images were obtained after intravenous administration of Gd-DTPA (Magnevist; Bayer HealthCare Pharmaceuticals,

Wayne, New Jersey). FDG-PET images were obtained on a 4-MDCT PET/CT scanner (GE Healthcare). One hour after IV injection of 20 mCi of FDG, noncontrast CT images were obtained for attenuation correction and fusion with emission PET images. A series of overlapping PET images was then obtained. CT images were coregistered and fused with emission PET images.<sup>11</sup> The maximum standard uptake value (SUV) within an ROI drawn around the lesion was calculated. SUV maximum values of >3.0 were defined as a positive signal. SPECT scanning was performed after IV injection of 3 mCi of thallium 201 as previously described.<sup>12</sup>

For ASL, imaging was achieved with pseudocontinuous labeling<sup>13</sup> and an interleaved stack of variable-attenuation, spiral, fast spin-echo sequence. Eight spiral interleaves were performed to achieve an in-plane resolution of 3.7 mm, and forty 4-mm axial sections were acquired. A postlabeling delay of 1.5 seconds and a labeling duration of 1.5 seconds were chosen.<sup>14</sup> Background suppression was performed with selective and nonselective inversion pulses applied at optimized times.<sup>15,16</sup> Three averages of label and control images were performed and then automatically subtracted. An additional reference image with a single saturation applied 2 seconds before imaging was also acquired to enable flow quantification. Quantification of blood flow was performed by using previously published methods.<sup>17</sup>

For ASL, positivity was determined by the neuroradiologist (D.H.) by visual inspection according to routine clinical practice. There have been no clinically used defined thresholds for quantitative measurements of blood flow to differentiate tumor and nontumor tissue, and calculated thresholds by using the same dataset would necessarily bias toward maximum accuracy.

### Image-Guided Stereotactic Biopsy

The target location for biopsy was determined by the neurosurgeons (C.C.C., P.C.W., E.K.) and was performed as previously described.<sup>10</sup> The Riechert frame was used in all biopsies. Biopsies were performed by using standard Nashold needles with a 10-mm side-cutting window (Integra LifeSciences, Plainsboro, NJ). To determine biopsy trajectories, we fused CE-MR imaging, PET, SPECT, and ASL by using Inomed software (Stereoplan Plus, Freiburg, Germany). Using these

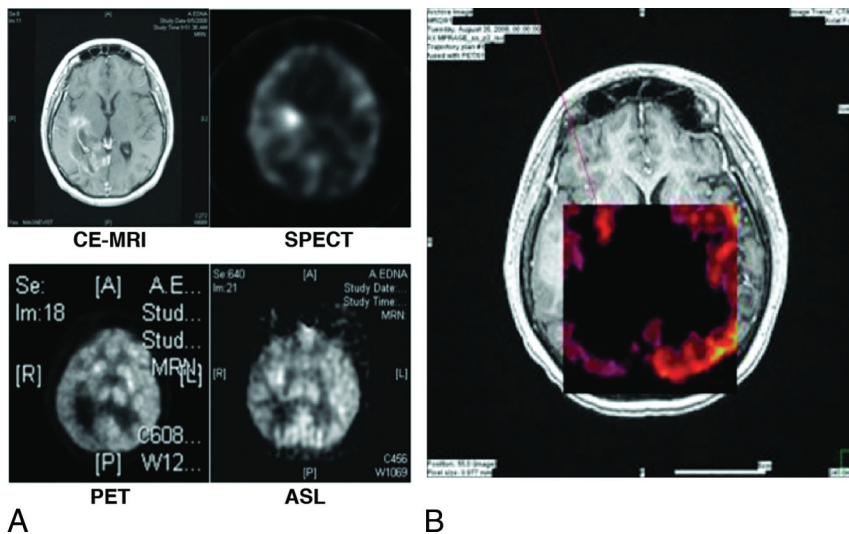


**FIG 1.** Individual images (A) CE MR imaging, thallium SPECT, FDG-PET, and ASL-MR imaging, and fused images (B) overlaid on CE-MR imaging. Red line represents the biopsy trajectory.

**Table 2: Accuracy, sensitivity, specificity, PPV, and NPV for each imaging modality**

	CE-MRI	PET	SPECT	MR ASL
Accuracy	46.2%	78.6%	57.1%	92.9%
Sensitivity	—	83.3%	50.0%	83.3%
Specificity	—	75.0%	62.5%	100.0%
PPV	—	71.4%	50.0%	100.0%
NPV	—	85.7%	62.5%	88.9%

**Note:** — indicates unable to calculate; CE-MRI were all positive for tumor progression.

**Table 3: Accuracy, sensitivity, specificity, PPV, and NPV<sup>a</sup>**

	PET or ASL +	PET or SPECT +	SPECT or ASL +	Any One +
Accuracy	85.7%	71.4%	71.4%	71.4%
Sensitivity	100.0%	100.0%	66.7%	100.0%
Specificity	75.0%	50.0%	62.5%	50.0%
PPV	75.0%	60.0%	57.1%	60.0%
NPV	100.0%	100.0%	71.4%	100.0%

<sup>a</sup> Positive = 1 modality positive.

reconstructions, we selected biopsy trajectories to afford sampling of CE-MR imaging, PET, SPECT, and ASL regions positive for tumor progression. To maximize the volume of tumor sampled, we planned a linear trajectory to allow serial sampling through the largest diameter of the tumor based on the imaging technique with the largest signal. In all cases, the region of biopsy was positive in at least 1 of the imaging modalities. While positivity differed among modalities within a single region, in no cases did 2 different modalities define distinct regions as scoring positive. For instance, there were no cases in which 1 region of the tumor scored positive for ASL while another scored positive for PET.

Pathology results were reviewed by a board-certified neuropathologist as a part of standard patient care. In accordance with the standard clinical practice, patients were classified as having tumor progression if the neuropathologist identified any histologic evidence of viable tumor. Patients were classified as having radiation necrosis only when no evidence of viable tumor was found by the neuropathologist. Results were reviewed with the neuropathologist at the tumor conference to confirm that the diagnosis stated in the formal pathology report was accurate.

## Statistical Analysis

Sensitivity, specificity, positive predictive value (PPV), and negative predictive value (NPV) were calculated for each imaging technique (CE-MR imaging, FDG-PET, thallium SPECT, and ASL) as they related to the pathology findings. Accuracy for each technique was calculated as (true positives + true negatives)/(all positives + all negatives). Values were also calculated for combinations of 2 or all 3 modalities. More stringent criteria were defined as positive tumor recurrence if all modalities were positive for TP. Less stringent criteria for positivity were defined if at least 1 technique was positive for TP.

## RESULTS

Of 267 patients stereotactically biopsied between 2007 and 2011, 14 underwent CE-MR imaging, FDG-PET, thallium SPECT, and ASL before surgical biopsy for definitive tissue diagnosis. The demographics of the study population are shown in Table 1. The patient ages ranged from 46 to 79 years. There were 9 male and 5 female patients. The patients had cerebral metastases from a spectrum of primary sites, including 4 lung cancers, 2 breast cancers, 3 renal cell carcinomas, 4 melanomas, and 1 esophageal cancer. On the basis of the final pathology, 6 patients (42%) had tumor progression, while 8 (58%) developed radiation necrosis. A representative coregistration of the 4 imaging modalities and the definition of the stereotactic target are shown in Fig 1.

Accuracy for tumor recurrence in metastatic cancer was highest by using ASL (87%), followed by FDG-PET (73%) and SPECT (53%), and lowest for CE-MR imaging (50%). Sensitivity was highest for ASL and PET (71%) and lowest for SPECT (43%). ASL had a specificity of 100%, while PET and SPECT were 75% and 63%, respectively. ASL also had the highest PPV (100%) and NPV (89%), whereas SPECT had the lowest (PPV, 50%; NPV, 63%). For FDG-PET, PPV was 71% and NPV was 86%. Results are summarized in Table 2. Although not used in the current analysis, quantitative values for ASL analyses are included in the On-line Table for reference.

For both positive and negative results, ASL and PET measures were in agreement 74% of the time; ASL and SPECT, 64%; and PET and SPECT, 50%. Agreement among all 3 modalities was 43%. When ASL-PET, PET-SPECT, and all 3 were in agreement, the accuracy was 100% in all cases. Accuracy was 93% when ASL and SPECT were in agreement.

A combination of different modalities did not result in higher accuracy than ASL alone when positivity was defined as a positive result in any 1 of a combination of 2 or all 3 modalities (Table 3). Sensitivity and NPV were both 100% when at one of modality (PET, ASL, or SPECT) was positive. However, specificity and PPV were lower than those for ASL alone at 75% and 50% for specificity and 75% and 66.7% for PPV, respectively. SPECT or ASL yielded lower predictive values for all



measures relative to ASL alone. The combination of all 3 modalities also had high sensitivity and NPV (100%) but low specificity and PPV (50% and 60%).

If positivity was defined more stringently as a positive result in both modalities, specificity increased to 100% for all combinations, which did not differ from findings in ASL alone. However, sensitivities were low. When both ASL and PET-positive, sensitivity = 67%; when both ASL and SPECT were positive, sensitivity = 50%; and when both SPECT and PET were positive, sensitivity = 50%; and when all 3 were positive, sensitivity = 33%. PPV was 100% for all combinations, but NPVs were all  $\leq 80\%$ . The accuracy of any of the combinations was never higher than that of ASL alone. See Table 4 for a summary.

### Illustrative Cases

**Case 1: Radiation Necrosis.** A 69-year-old man had a solitary renal cell carcinoma metastasis to the periventricular white matter of

the posterior left lateral horn. Progression on CE-MR imaging was noted 13 months following radiosurgery (18 Gy in a single fraction, Fig 2A). Physiologic imaging findings were only positive on SPECT. Biopsy revealed radiation necrosis.

**Case 2: Tumor Recurrence.** A 46-year-old woman had metastatic breast cancer metastasis to the right cerebellum. Progression on CE-MR imaging was noted 9 months following radiosurgery (5 Gy  $\times$  5 fractions, Fig 2B). Physiologic imaging showed positive signals on ASL and PET (SUV = 6.6). Thallium SPECT findings were negative. Biopsy revealed tumor recurrence.

**Case 3: Tumor Recurrence.** A 58-year-old man had a solitary melanoma metastasis to the right inferior frontal cortex. Progression on CE-MR imaging was noted 22 months after SRS (18 Gy in a single fraction, Fig 2C). Physiologic imaging findings were positive on PET only (SUV = 10.7). Biopsy revealed tumor recurrence.

**Table 4: Accuracy, sensitivity, specificity, PPV, and NPV<sup>a</sup>**

	PET and ASL +	PET and SPECT +	SPECT and ASL +	All +
Accuracy	85.7%	78.6%	78.6%	71.4%
Sensitivity	66.7%	50.0%	66.7%	100.0%
Specificity	100.0%	100.0%	100.0%	100.0%
PPV	100.0%	100.0%	100.0%	100.0%
NPV	80.0%	72.7%	72.7%	66.7%

<sup>a</sup> Positive = all modalities positive.

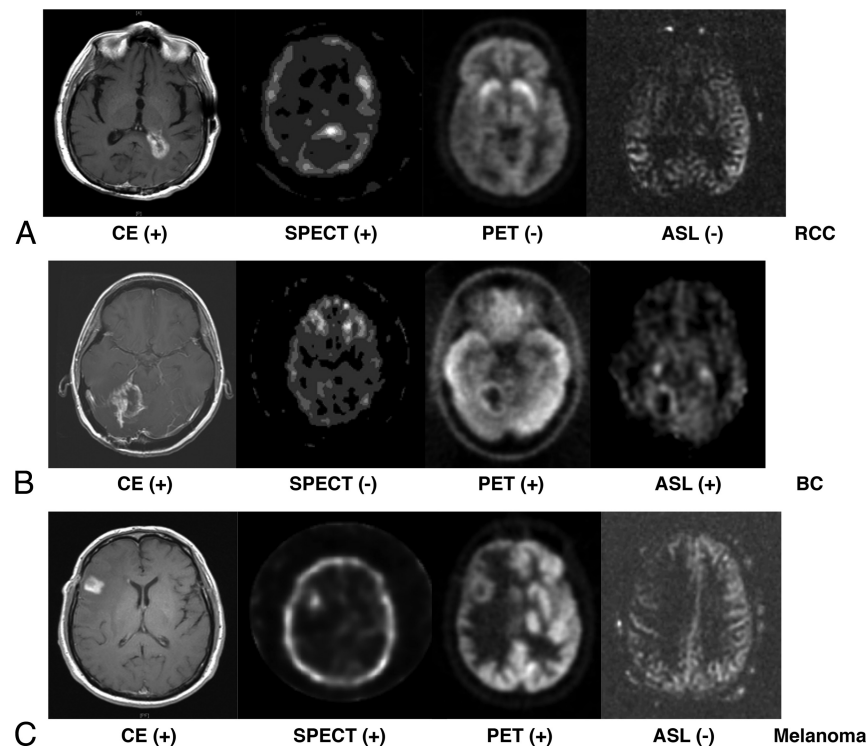


**FIG 2.** CE-MR imaging, thallium SPECT, FDG-PET, and ASL-MR images from case 1 (A) with metastatic renal cell carcinoma to periventricular white matter of the posterior left lateral horn. CE-MR imaging shows new enhancement in the region treated. SPECT was positive while PET and ASL were negative for tumor recurrence. Biopsy of the target region indicated radiation necrosis in case 2 (B) with metastatic breast cancer to the right cerebellum. CE-MR imaging shows new enhancement in the region treated. PET (SUV = 6.6) and ASL were positive for tumor recurrence. Biopsy of the target region indicated tumor recurrence in case 3 (C) with metastatic melanoma to the right inferior frontal cortex. Only PET was positive for tumor recurrence (SUV = 10.7). Biopsy of the target region indicated tumor recurrence.

### DISCUSSION

This study compares the diagnostic utility of FDG-PET, thallium SPECT, and ASL in the post-SRS setting by using pathologic diagnoses secured through targeted biopsies as the criterion standard. We analyzed imaging results in 14 patients with cerebral metastases who underwent SRS and were biopsied after clinical or radiographic progression. Only 46% of patients with enlarging contrast enhancement on MR imaging had tumor progression confirmed by histopathology. This finding highlights the inadequacy of conventional MR imaging in this setting. Of the 3 physiologic imaging modalities studied, ASL exhibited the highest level of sensitivity and specificity in terms of discriminating between RN and TP. Combining imaging modalities did not substantially improve the diagnostic utility of ASL (Table 3).

In clinical practice, FDG-PET and thallium SPECT are often used for detection of intracranial lesions. In prior studies, the sensitivity and specificity of FDG-PET for discriminating TP and RN for primary gliomas ranged from 77% to 81% and 63% to 90%, respectively.<sup>18-20</sup> Sensitivity and specificity for brain metastases were 86% and 80%.<sup>18</sup> These results are largely in line with those observed in this study (sensitivity 83%, specificity 75%). However, thallium SPECT results reported in this study (sensitivity 50%, specificity 63%) were markedly lower than those previously reported (specificity and sensitivity values of 82.7%–91% and 82.8%–90% for primary gliomas and metastases<sup>21,22</sup>). In fact, a recent review reported that SPECT was superior to other imaging modalities for differentiating radiation necrosis and TP in primary gliomas.<sup>23</sup>

However, no studies have directly compared SPECT and ASL in the same patient population, to our knowledge.

Although ASL perfusion is not yet widely used clinically in the setting of neoplasm, perfusion MR imaging such as dynamic susceptibility contrast MR imaging has been of recent interest for the investigation of brain tumors. Like ASL, DSC measures brain perfusion but relies on dynamic measurement of intravenous contrast agents.<sup>23</sup> Because intravenous contrast agents are typically administered in the oncologic population, each additional scan that requires contrast compounds the risk of morbidity. In terms of the diagnostic utility of the 2 MR perfusion modalities, studies directly comparing CBF values in ASL and DSC for tumor,<sup>17,24</sup> ischemic tissue, and normal brain have consistently noted<sup>24</sup> high correlations. For brain metastases, DSC-MR imaging yielded sensitivity and specificity values from 70% to 100% and 95.2% to 100% for differentiation of necrosis and tumor recurrence.<sup>25,26</sup> In differentiating tumor recurrence and radiation necrosis or pseudoprogression of primary gliomas, direct comparison between ASL and DSC-MR imaging showed no statistical significance, with sensitivity and specificity values of 79%–94% and 64%–88%.<sup>20,27</sup> In terms of detection of gliomas and metastases, ASL and DSC-MR imaging also showed similar diagnostic yields.<sup>28,29</sup> However, ASL has the advantages of better signal-to-noise ratio, fewer distortion effects secondary to hemorrhage, and the potential for quantification.<sup>17</sup> More definitive studies comparing the 2 modalities will be needed in the patient population with postradiation metastasis. Furthermore, larger studies using ASL for tumor identification will be necessary to establish generalizable thresholds for interpretation of quantitative ASL values.

Supporting the idea that perfusion imaging would be an ideal technique for differentiation of tumor progression and radiation necrosis is the assumption that tumor has sufficiently more vascularity than fibrous or necrotic tissue. Likewise, FDG-PET positivity depends on glucose uptake. If the metabolism of the tumor does not require glucose uptake, then FDG-PET will be falsely negative. Thallium SPECT positivity is determined by the presence of functional sodium-potassium adenosine triphosphatase. If this transporter is not active in the tumor, thallium SPECT findings will be falsely positive. Reliable detection of tumor post-radiation may require different functional modalities, depending on specific characteristics of the tumor. Furthermore, a fundamental question in imaging revolves around the resolution and sensitivity of the imaging technique relative to the strength of signal based on size, attenuation, and intensity of the measure of interest of a tumor.

With regard to the use of image-guided stereotactic biopsy, possible errors of coregistration remain an important consideration. However, our method of registration and biopsy has been shown, by our group and others, to be highly accurate. Nondiagnostic tissue samples occurred at a rate of 4.6%–5%.<sup>10,30</sup>

In the current practice setting, there is a high degree of subjectivity in the management of patients with cerebral metastasis who have radiographic and/or clinical progression after SRS. While our study is limited by the small sample size, it represents a systematic effort to address a clinically important question. Most studies investigating posttreatment imaging use presumptive diagnoses or have only a subset of patients with histology. Another

limitation is the heterogeneity of metastatic tumor types represented in this study. Metastases may exhibit varying levels of flow depending on their primary location and individual variability in tumor physiology. For example, melanomas have a short T1, and accumulation of the ASL signal can be attenuated.<sup>31</sup> Furthermore, flow in regions with reduced activity due to radiation or vascular disease may be underestimated by ASL due to delayed arrival of arterial blood. Such underestimation might be addressed by newer ASL techniques that can label for longer and also measure the arterial transit delay.<sup>32,33</sup> However, despite the predicted underestimation of effect size given the heterogeneity of our sample, ASL appeared to provide useful diagnostic information. A larger study comparing perfusion imaging (ASL and DSC) with tissue diagnosis would be of importance to validate the present results and has the potential to fundamentally alter our clinical practice in the surveillance and management of patients with cancer after SRS treatment.

## CONCLUSIONS

Our results suggest that ASL offers a noninvasive method in the discrimination of RN from TP in patients with cerebral metastasis who underwent SRS. Results from the present study provide a basis for future prospective studies with larger sample sizes to validate the use of ASL in this setting.

**Disclosures:** Anand Mahadevan—UNRELATED: Board Membership: Radiosurgery Society, Comments: Nonpaid board member, President; Royalties: UptoDate. David Hackney—UNRELATED: Consultancy: University of California, San Francisco, Comments: I am a consultant to the brain tumor group, serving on the External Advisory Board for their brain tumor Specialized Program of Research Excellence and Program Project. Thus, my work is relevant to the broad issue of brain tumor imaging, but it does not influence what I might say about this study. I am paid an honorarium for my participation in the annual Educational Advisory Board meeting in San Francisco. Peter C. Warnke—UNRELATED: Consultancy: Gerson Lehrman Group (consulting firm). Ekkehard Kasper—UNRELATED: Expert Testimony: McKeen & Associates; Detroit, Michigan, Comments: occasional legal expert witness work for this Detroit law firm. Eric T. Wong—UNRELATED: Grants/Grants Pending: AngioChem,\* Astra-Zeneca,\* Cephalon,\* Eli Lilly,\* Northwest Biotherapeutics,\* Novartis,\* Novocure,\* Pfizer,\* Plexxicon.\* \*Money paid to the institution.

## REFERENCES

1. Chernov M, Hayashi M, Izawa M, et al. **Differentiation of the radiation-induced necrosis and tumor recurrence after gamma knife radiosurgery for brain metastases: importance of multi-voxel proton MRS.** *Minim Invasive Neurosurg* 2005;48:228–34 [CrossRef Medline](#)
2. Shah R, Vattoth S, Jacob R, et al. **Radiation necrosis in the brain: imaging features and differentiation from tumor recurrence.** *Radiographics* 2012;32:1343–59 [CrossRef Medline](#)
3. Stockham AL, Tievsky AL, Koefman SA, et al. **Conventional MRI does not reliably distinguish radiation necrosis from tumor recurrence after stereotactic radiosurgery.** *J Neurooncol* 2012;109:149–58 [CrossRef Medline](#)
4. Doms GC, Hecht S, Brant-Zawadzki M, et al. **Brain radiation lesions: MR imaging.** *Radiology* 1986;158:149–55 [CrossRef Medline](#)
5. Rahmathulla G, Marko NF, Weil RJ. **Cerebral radiation necrosis: a review of the pathobiology, diagnosis and management considerations.** *J Clin Neurosci* 2013;20:485–502 [CrossRef Medline](#)
6. Chao ST, Ahluwalia MS, Barnett GH, et al. **Challenges with the diagnosis and treatment of cerebral radiation necrosis.** *Int J Radiat Oncol Biol Phys* 2013;87:449–57 [CrossRef Medline](#)
7. Woodworth GF, McGirt MJ, Samdani A, et al. **Frameless image-guided stereotactic brain biopsy procedure: diagnostic yield, surgical morbidity, and comparison with the frame-based technique.** *J Neurosurg* 2006;104:233–37 [CrossRef Medline](#)

8. Sawin PD, Hitchon PW, Follett KA, et al. **Computed imaging-assisted stereotactic brain biopsy: a risk analysis of 225 consecutive cases.** *Surg Neurol* 1998;49:640–49 CrossRef Medline
9. McGirt MJ, Woodworth GF, Coon AL, et al. **Independent predictors of morbidity after image-guided stereotactic brain biopsy: a risk assessment of 270 cases.** *J Neurosurg* 2005;102:897–901 CrossRef Medline
10. Waters JD, Gonda DD, Reddy H, et al. **Diagnostic yield of stereotactic needle-biopsies of sub-cubic centimeter intracranial lesions.** *Surg Neurol Int* 2013;4:S176–81 CrossRef Medline
11. Williams G, Kolodny GM. **Method for decreasing uptake of 18F-FDG by hypermetabolic brown adipose tissue on PET.** *AJR Am J Roentgenol* 2008;190:1406–09 CrossRef Medline
12. Hill TC, Holman BL, Lovett R, et al. **Initial experience with SPECT (single-photon computerized tomography) of the brain using N-isopropyl I-123 p-iodoamphetamine: concise communication.** *J Nucl Med* 1982;23:191–95 Medline
13. Dai W, Garcia D, de Bazelaire C, et al. **Continuous flow-driven inversion for arterial spin labeling using pulsed radio frequency and gradient fields.** *Magn Reson Med* 2008;60:1488–97 CrossRef Medline
14. Alsop DC, Detre JA. **Reduced transit-time sensitivity in noninvasive magnetic resonance imaging of human cerebral blood flow.** *J Cereb Blood Flow Metab* 1996;16:1236–49 Medline
15. Ye FQ, Frank JA, Weinberger DR, et al. **Noise reduction in 3D perfusion imaging by attenuating the static signal in arterial spin tagging (ASSIST).** *Magn Reson Med* 2000;44:92–100 CrossRef Medline
16. Maleki N, Dai W, Alsop DC. **Optimization of background suppression for arterial spin labeling perfusion imaging.** *MAGMA* 2012;25:127–33 CrossRef Medline
17. Järnum H, Steffensen EG, Knutsson L, et al. **Perfusion MRI of brain tumours: a comparative study of pseudo-continuous arterial spin labelling and dynamic susceptibility contrast imaging.** *Neuroradiology* 2010;52:307–17 CrossRef Medline
18. Chao ST, Suh JH, Raja S, et al. **The sensitivity and specificity of FDG PET in distinguishing recurrent brain tumor from radionecrosis in patients treated with stereotactic radiosurgery.** *Int J Cancer* 2001;96:191–97 CrossRef Medline
19. Tan H, Chen L, Guan Y, Lin X. **Comparison of MRI, F-18 FDG, and 11C-choline PET/CT for their potentials in differentiating brain tumor recurrence from brain tumor necrosis following radiotherapy.** *Clin Nucl Med* 2011;36:978–81 CrossRef Medline
20. Ozsunar Y, Mullins ME, Kwong K, et al. **Glioma recurrence versus radiation necrosis? A pilot comparison of arterial spin-labeled, dynamic susceptibility contrast enhanced MRI, and FDG-PET imaging.** *Acad Radiol* 2010;17:282–90 CrossRef Medline
21. Serizawa T, Saeki N, Higuchi Y, et al. **Diagnostic value of thallium-201 chloride single-photon emission computerized tomography in differentiating tumor recurrence from radiation injury after gamma knife surgery for metastatic brain tumors.** *J Neurosurg* 2005;102(suppl):266–71 CrossRef Medline
22. Matsunaga S, Shuto T, Takase H, et al. **Semiquantitative analysis using thallium-201 SPECT for differential diagnosis between tumor recurrence and radiation necrosis after gamma knife surgery for malignant brain tumors.** *Int J Radiat Oncol Biol Phys* 2013;85:47–52 CrossRef Medline
23. Shah AH, Snelling B, Bregy A, et al. **Discriminating radiation necrosis from tumor progression in gliomas: a systematic review what is the best imaging modality?** *J Neurooncol* 2013;112:141–52 CrossRef Medline
24. Jiang J, Zhao L, Zhang Y, et al. **Comparative analysis of arterial spin labeling and dynamic susceptibility contrast perfusion imaging for quantitative perfusion measurements of brain tumors.** *Int J Clin Exp Pathol* 2014;7:2790–99 Medline
25. Hoefnagels FW, Lagerwaard FJ, Sanchez E, et al. **Radiological progression of cerebral metastases after radiosurgery: assessment of perfusion MRI for differentiating between necrosis and recurrence.** *J Neurol* 2009;256:878–87 CrossRef Medline
26. Mitsuya K, Nakasu Y, Horiguchi S, et al. **Perfusion weighted magnetic resonance imaging to distinguish the recurrence of metastatic brain tumors from radiation necrosis after stereotactic radiosurgery.** *J Neurooncol* 2010;99:81–88 CrossRef Medline
27. Choi YJ, Kim HS, Jahng GH, et al. **Pseudoprogression in patients with glioblastoma: added value of arterial spin labeling to dynamic susceptibility contrast perfusion MR imaging.** *Acta Radiol* 2013;54:448–54 CrossRef Medline
28. Lehmann P, Monet P, de Marco G, et al. **A comparative study of perfusion measurement in brain tumours at 3 Tesla MR: arterial spin labeling versus dynamic susceptibility contrast-enhanced MRI.** *Eur Neurol* 2010;64:21–26 CrossRef Medline
29. Warmuth C, Gunther M, Zimmer C. **Quantification of blood flow in brain tumors: comparison of arterial spin labeling and dynamic susceptibility-weighted contrast-enhanced MR imaging.** *Radiology* 2003;228:523–32 CrossRef Medline
30. Tilgner J, Herr M, Ostertag C, Volk B. **Validation of intraoperative diagnoses using smear preparations from stereotactic brain biopsies: intraoperative versus final diagnosis—influence of clinical factors.** *Neurosurgery* 2005;56:257–65; discussion 257–65 CrossRef Medline
31. Isiklar I, Leeds NE, Fuller GN, et al. **Intracranial metastatic melanoma: correlation between MR imaging characteristics and melanin content.** *AJR Am J Roentgenol* 1995;165:1503–12 CrossRef Medline
32. Dai W, Shankaranarayanan A, Alsop DC. **Volumetric measurement of perfusion and arterial transit delay using Hadamard encoded continuous arterial spin labeling.** *Magn Reson Med* 2013;69:1014–22 CrossRef Medline
33. Dai W, Robson PM, Shankaranarayanan A, et al. **Reduced resolution transit delay prescan for quantitative continuous arterial spin labeling perfusion imaging.** *Magn Reson Med* 2012;67:1252–65 CrossRef Medline